for pseudodegenerate electronic states assuming linear vibronic coupling and identical adiabatic force constants for both the ground and the first excited states is given by

$$E_{\pm} = \tfrac{1}{2}kS'^2 \pm \sqrt{(\Delta^2 + a^2S'^2)} \quad (8)$$

$E_{\pm}$ is the energy of the upper (+) and lower (-) energy surfaces, k is the adiabatic or "classical" force constant of the active vibrational mode with symmetry coordinate S', 2Δ is the energy difference between the nondegenerate states of an undistorted molecule, and a is the linear vibronic coupling constant, $\langle\psi_+|(\partial H^e/\partial S_i')_0|\psi_-\rangle$. (Actually, this equation is identical in form with that derived for the effects of first-order spin-orbit coupling on orbitally degenerate states, except that λ, the spin-orbit coupling constant, replaces 2Δ. The removal of electronic degeneracy is then a result of spin-orbit coupling rather than chemical substitution.[63,64]) It is easily shown that if $2\Delta > 2a^2/k$, both curves are parabolas and pseudo-Jahn-Teller distortion does not occur. Otherwise, the lower energy surfaces will have equivalent minima (e.g., for an isolated molecule; see the solid curves in Figure 3) at

$$S_{pjt} = \pm\sqrt{(a^2/k^2 - \Delta^2/a^2)} \quad (9)$$

and distortion from the symmetrical geometry will be spontaneous.

Unfortunately, eq 8 contains three parameters that are extremely difficult to obtain experimentally. Nevertheless, it is possible to derive an equivalent expression of $E_{\pm}$ in terms of parameters that are much more amenable to experimental determination

$$E_{\pm} = (S'/S_{pjt})^2(\sqrt{WB} - B) \pm \tfrac{1}{2}\sqrt{W^2 + (4W/S_{pjt}^2)(S'^2 - S_{pjt}^2)(\sqrt{WB} - B)} \quad (10)$$

W, the transition energy between the ^{2}A ground and ^{2}B first excited electronic state, can be obtained easily from near-infrared visible spectroscopic measurements, B, the barrier height between the ground-state minima, can be obtained from ESR bandwidth experiments,[50] and S_{pjt} can be obtained from very low-temperature X-ray experiments.[65] Three other useful equations follow from this derivation

$$2\Delta = W - 2\sqrt{WB} \quad (11)$$

$$k = (2/S_{pjt}^2)(\sqrt{WB} - B) \quad (12)$$

$$a = S_{pjt}^{-1}\sqrt{W(\sqrt{WB} - B)} \quad (13)$$

For $[Cu(bpy)_2(ONO)]NO_3$, W = 9620 cm^{-1} [6] and S_{pjt} = 0.355 Å. Assuming a reasonable value of B, say, 500 cm^{-1}, from eq 11-13, 2Δ = 5230 cm^{-1}, k = 26 900 cm^{-1} Å^{-2} (or 0.53 mdyn Å^{-1}), and a = 11 370 cm^{-1} Å^{-1}, and are all very reasonable values.[66,67]

For a given series of $[CuL_2(OXO)]Y$ complexes, the values of 2Δ will be proportional to the ligand strengths of the different OXO groups, being zero if OXO is bpy or phen. Attempts to obtain a relative ranking of ligand strengths by measuring the S_{pjt} and B values for a variety of these complexes by using low-temperature X-ray diffraction and ESR techniques are now in progress at the University of Puerto Rico and the University of Iowa.

Acknowledgment. We thank Sten Samson, Richard Marsh, and William Schaefer at the California Institute of Technology and Hans Bürgi, University of Bern, for helpful discussions, the Molecular Structure Corporation, College Station, TX, for their help in obtaining the 165 and 296 K data for $[Cu(bpy)_2(ONO)]NO_3$, and Karl Seff, University of Hawaii, for allowing us to obtain the 295 K data for $[Zn(bpy)_2(ONO)]NO_3$. B.D.S. acknowledges support as a Myron A. Bantrell Research Fellow in Chemical Catalysis at the California Institute of Technology (1980-83) and support for an upgrade of the X-ray Facility by the National Science Foundation (Grant No. CHE8219039).

Supplementary Material Available: Tables of U_{ij}'s (S1, S2, and S3), bond lengths and angles involving hydrogen atoms (S4), and analysis of Gaussian ellipsoids (S5) (13 pages); listing of observed and calculated structure factors (S6, S7, S8, S9, and S10) (61 pages). Ordering information is given on any current masthead page.

(63) Ballhausen, C. J. *Theor. Chem. Acta* **1965**, *3*, 368.
(64) Bacci, M. *J. Chem. Educ.* **1982**, *59*, 816.
(65) Vibrational zero-point energies have been neglected in eq 10; the experimentally determined energy values of W and B should be incremented accordingly. A reasonable value for the $[CuL_2(OXO)]Y$ systems is ca. 275 cm^{-1}.
(66) Nakamoto, K. *Infrared and Raman Spectra of Inorganic and Coordinated Compounds*; Wiley: New York, 1986; p 229.
(67) Deeth, R. J.; Hitchman, M. A. *Inorg. Chem.* **1986**, *25*, 1225.

Crystal and Molecular Structure of Bis(imidazole)(*meso*-tetraphenylporphinato)iron(III) Chloride. A Classic Molecule Revisited

W. Robert Scheidt,* Sarah R. Osvath, and Young Ja Lee

Contribution from the Department of Chemistry, University of Notre Dame, Notre Dame, Indiana 46556. *Received October 15, 1986*

Abstract: The crystal and molecular structure of the low-spin compound $[Fe(TPP)(HIm)_2]Cl$ has been determined by X-ray diffraction methods. The asymetric unit of structure contains two independent half $[Fe(TPP)(HIm)_2]^+$ ions. Each ion has required inversion symmetry, and the two axial ligand planes within each ion are thus parallel. The two ions have distinctly different orientations of the imidazoles with respect to the porphyrin and give rise to two overlapping EPR signals. The differing orientations of the axial ligands also lead to changes in the rhombicity of the coordination bond parameters, a previously unrecognized effect in low-spin ferric porphyrinates. The differing orientations of the axial ligands appear to result from participation in an extended hydrogen bonding network in the crystalline lattice. Crystal data: space group $P\bar{1}$, Z = 2, a = 13.331 (2) Å, b = 17.688 (3) Å, c = 11.213 (2) Å, α = 107.99 (1)°, β = 94.70 (1)°, and γ = 69.68 (1)° at 292 K.

We have been investigating the effects of, and the control of, specific axial ligand orientations on metalloporphyrin physical properties. Work to date reveals that effects appearing to be describable in terms of axial ligand orientations are significant. A convenient method for describing the precise axial ligand orientation in metalloporphyrins, for planar axial ligands, is to

0002-7863/87/1509-1958$01.50/0

calculate the dihedral angle between the axial ligand plane and a coordinate plane defined by a porphinato nitrogen atom, the metal atom, and the axial ligand donor atom. This orientation angle, first used by Hoard et al.,[1] is commonly called ϕ and was originally used in describing, in exquisite detail, the structure of the $[Fe(TPP)(HIm)_2]^+$ ion.[2] This complex, the first low-spin iron porphyrinate to be structurally characterized, has two different imidazole orientations, the first with $\phi = 18°$ and the second with $\phi = 39°$. These two distinct orientations of the axial ligands were associated with different axial Fe–N bond lengths of 1.957 (4) and 1.991 (5) Å. The less sterically favored imidazole ($\phi = 18°$) was found to have the longer coordination bond. Subsequent[3] structural investigations of bis(imidazole) complexes have shown that the longer axial bond length is always associated with the smaller (less favorable) value of ϕ. It is important to note that the value of ϕ does not appear to be a predictor of the *absolute* value of the axial bond length.

We have demonstrated that changes in specific axial ligand orientation are consistent with different spin states in iron(III) derivatives. We have shown that $[Fe(OEP)(3\text{-}ClPy)_2]ClO_4$[4,5] and $[Fe(TPP)(NCS)(Py)]$[6,7] display different spin states in different crystalline forms. Structural analysis shows that in all cases, the complex with the smaller value of ϕ corresponds to the state of higher spin. In principle, such effects could be used as a control mechanism for the choice of spin state.

We have also carried out a theoretical investigation[8] of imidazole orientation preferences in metalloporphyrin derivatives; the observed preference of small ϕ values was found to correlate with an electronic effect, namely ϕ-dependent π-bonding in which the imidazole ligand π-donates to empty metal p orbitals and empty or partially filled d orbitals.

In recent work,[9] we have examined the effect of axial ligand orientation on the EPR spectra of low-spin iron(III) derivatives. For bis(imidazole) complexes, we now believe that the presence of an unusual EPR signal, the so-called strong g_{max} spectrum, is the result of a perpendicular alignment of the two imidazole planes. The structure of one such complex, $[Fe(TPP)(2\text{-}MeHIm)_2]ClO_4$, is reported[10] in the following paper. As part of that EPR and Mössbauer investigation,[9] we wished to obtain the spectrum of a compound that had an intermediate value for the dihedral angle between the imidazole planes. The $[Fe(TPP)(HIm)_2]^+$ ion, as reported by Hoard et al.,[1] appeared to be an ideal case. However, our attempts to prepare a crystalline sample of $[Fe(TPP)(HIm)_2]Cl$ did not yield a sample that was identical with that reported previously.[1] (A solid sample is needed to eliminate any ambiguity in the value of the dihedral angles.) The crystalline complex that we obtained has the stoichiometry $[Fe(TPP)(HIm)_2]Cl\cdot CHCl_3\cdot H_2O$ rather than that of $[Fe(TPP)(HIm)_2]Cl\cdot CH_3OH$ as originally reported. Most significantly, this new crystalline sample of $[Fe(TPP)(HIm)_2]Cl$ displays two overlapping "normal" low-spin EPR spectra with $g_z = 3.00$, $g_y \approx 2.2$, $g_x = 1.47$ and $g_z = 2.84$, $g_y = 2.32$, $g_x = 1.59$. Frozen solutions of the compound yield an EPR signal with $g_z = 2.87$, $g_y = 2.29$, and $g_x = 1.56$.[11] We have determined the molecular and crystal structure of $[Fe(TPP)(HIm)_2]Cl\cdot CHCl_3\cdot H_2O$ in order to understand the origin of the EPR spectra.

This new crystalline phase of $[Fe(TPP)(HIm)_2]Cl$ is found to have significant differences in structure from that reported by Hoard et al.[1] This new phase has two independent ions in the crystal. Each $[Fe(TPP)(HIm)_2]^+$ ion has two imidazole ligands with parallel planes. Most significantly, the ϕ orientation angles for the two ions are quite different. Moreover, the Fe–N_p bond distances show a rhombic distortion that appears to be related to the imidazole ligand orientations. Reasons for the two distinct orientations of the axial ligands are suggested from an examination of the crystal structure of $[Fe(TPP)(HIm)_2]Cl\cdot CHCl_3\cdot H_2O$. These features also suggest some ideas concerning the relative energetics of imidazole ligand orientation. Hence it appeared to us that the structural features of this new crystalline form of $[Fe(TPP)(HIm)_2]Cl$ are as illuminating as that of the original report. We report herein our revisit to the molecular and crystal structure of low-spin $[Fe(TPP)(HIm)_2]Cl$.

Experimental Section

A variety of attempts to prepare crystalline samples of the $[Fe(TPP)(HIm)_2]Cl$ phase reported by Hoard et al.[1] were unsuccessful. These resulting powder or microcrystalline samples all showed normal EPR spectra with small variations in the EPR parameters. Some samples showed overlapping EPR signals. All these attempts utilized CH_3OH in some way in the crystallizing procedure. Crystals were obtained by reaction of 35 mg of Fe(TPP)Cl (0.05 mmol) and 0.30 mmol of recrystallized imidazole dissolved in 4 mL of chloroform. The resulting solution was left to crystallize by allowing a 1:2 chloroform:hexane mixture to diffuse into the solution. Single crystals were obtained in 3–4 days.

Crystals of $[Fe(TPP)(HIm)_2]Cl\cdot CHCl_3\cdot H_2O$ were examined on a CAD4 automated diffractometer. This examination established a two-molecule triclinic unit cell with space group $P1$ or $P\bar{1}$. A single-crystal specimen with dimensions of $0.05 \times 0.30 \times 0.43$ mm was used for data collection and cell constant determination. Least-squares refinement of the setting angles of 25 reflections with $22 < 2\theta < 28$ led to the following cell constants: $a = 13.331$ (2) Å, $b = 17.688$ (3) Å, $c = 11.213$ (2) Å, $\alpha = 107.99$ (1)°, $\beta = 94.70$ (1)°, and $\gamma = 69.68$ (1)°. For a cell content of $[Fe(TPP)(HIm)_2]Cl\cdot CHCl_3\cdot H_2O$, the calculated density was 1.377 g/cm^3; the experimental density was 1.35 g/cm^3. Intensity data were measured on the CAD4 diffractometer with graphite-monchromated Mo Kα radiation and θ–2θ scanning at the ambient laboratory temperature of 19 ± 1 °C. Four standard reflections were measured every 60 min to monitor the long-term stability of the experiment; no significant deviations were noted. Intensity data were reduced and a total of 5692 reflections having $(\sin\theta)/\lambda < 0.649$ Å^{-1} and $F_o > 3\sigma(F_o)$ were retained as observed. The structure was solved by a combination of Patterson methods and the direct methods program DIRDIF.[12] The Patterson map showed the heavy-atom vector 0.5, 0.5, 0.5; one cycle of DIRDIF with iron positions of 0, 0, 0 and $^1/_2$, $^1/_2$, $^1/_2$ in space group $P\bar{1}$, led to the positions of all heavy atoms of the two half ions. A subsequent difference Fourier synthesis led to the chloride ion and water molecule positions. It is to be noted that the irons are on special positions but the chloride ions (also two per unit cell) are located in general positions. After several cycles of full-matrix least-squares refinement, difference Fouriers showed the positions of all hydrogen atoms. These hydrogen atoms were included in all subsequent cycles of least-squares refinement as fixed contributors

(1) Collins, D. M.; Countryman, R.; Hoard, J. L. *J. Am. Chem. Soc.* **1972**, *94*, 2066–2072.

(2) Abbreviations used: TPP and OEP, dianions of *meso*-tetraphenylporphyrin and octaethylporphyrin; 2-MeHIm, 2-methylimidazole, HIm, imidazole; 1-MeIm, 1-methylimidazole; BzHim, benzimidazole; Py, Pyridine; 3-ClPy, 3-chloropyridine; N_p, porphinato nitrogen.

(3) (a) Little, R. G.; Dymock, K. R.; Ibers, J. A. *J. Am. Chem. Soc.* **1975**, *97*, 4532–4539. (b) Quinn, R.; Strouse, C. E.; Valentine, J. S. *Inorg. Chem.* **1983**, *22*, 3934–3940.

(4) A high-spin to low-spin thermal equilibrium is reported in the following: Scheidt, W. R.; Geiger, D. K.; Haller, K. J. *J. Am. Chem. Soc.* **1982**, *104*, 495–499.

(5) An intermediate-spin form of the complex is reported in the following: Scheidt, W. R.; Geiger, D. K.; Hayes, R. G.; Lang, G. *J. Am. Chem. Soc.* **1983**, *105*, 2625–2632.

(6) A low-spin form of the complex is given in the following: Scheidt, W. R.; Lee, Y. L.; Geiger, D. K.; Taylor, K.; Hatano, K. *J. Am. Chem. Soc.* **1982**, *104*, 3367–3374.

(7) A high-spin form of the complex is detailed in the following: Geiger, D. K.; Chunplang, V.; Scheidt, W. R. *Inorg. Chem.* **1986**, *25*, 4736–4741.

(8) Scheidt, W. R.; Chipman, D. M. *J. Am. Chem. Soc.* **1986**, *108*, 1163–1167.

(9) Walker, F. A.; Huynh, B. H.; Scheidt, W. R.; Osvath, S. R. *J. Am. Chem. Soc.* **1986**, *108*, 5288–5297.

(10) Scheidt, W. R.; Kirner, J. F.; Hoard, J. L.; Reed, C. A. *J. Am. Chem. Soc.*, following paper in this issue.

(11) Walker, F. A.; Reis, D.; Balke, V. L. *J. Am. Chem. Soc.* **1984**, *106*, 6888–6898.

(12) Buerskens, P. T.; Bosman, W. P.; Doesburg, H. M.; Gould, R. O.; van den Hark, Th. E. M.; Prick, P. A. J.; Noordik, J. H.; Buerskens, G.; Parthasarathi, V., Technical Report 1981/2, Crystallography Laboratory, Toernooiveld, Netherlands. Other programs used in this study included local modifications of Jacobson's ALLS, Zalkin's FORDAP, Busing and Levy's ORFFE and ORFLS, and Johnson's ORTEP2. Atomic form factors were from the following: Cromer, D. T.; Mann, J. B. *Acta Crystallogr., Sect. A* **1968**, *A24*, 321–323. Real and imaginary corrections for anomalous dispersion in the form factor of the iron and chlorine atoms were from the following: Cromer, D. T.; Liberman, D. J. *J. Chem. Phys.* **1970**, *53*, 1891–1898. Scattering factors for hydrogen were from the following: Stewart, R. F.; Davidson, E. R.; Simpson, W. T. *Ibid.* **1965**, *42*, 3175–3187. All calculations were performed on a VAX 11/730.

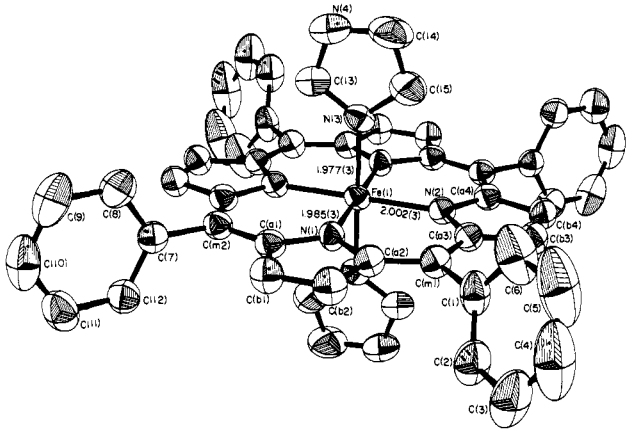

Figure 1. ORTEP2 drawing of the first $[Fe(TPP)(HIm)_2]^+$ ion. The atom labeling scheme for the crystallographically unique atoms is shown. The unique bond distances in the coordination group are given. Thermal ellipsoids are contoured at the 50% probability level.

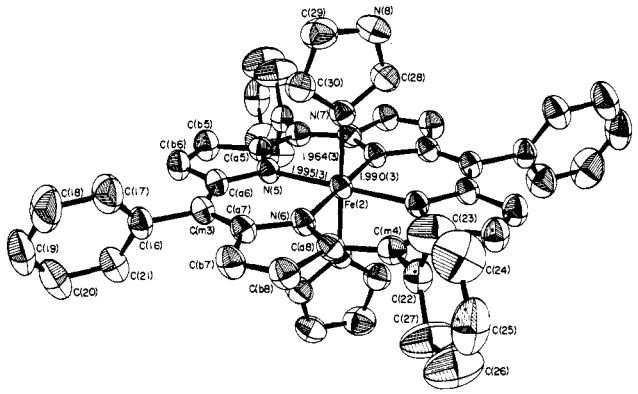

Figure 2. ORTEP2 drawing of the second $[Fe(TPP)(HIm)_2]^+$ ion. The same information as given in Figure 1 is displayed.

(C–H = 0.95 Å, N–H = 0.87 Å, and $B(H) = B(C, N, \text{or } O) + 1.0$ Å^2). The two hydrogen atoms of the water molecule were fixed at their Fourier map positions. Final cycles were carried out with anisotropic temperature factors for all heavy atoms. At convergence, the final discrepancy indices were $R_1 = 0.051$ and $R_2 = 0.063$[13] with an error of fit of 1.80. The final data/parameter ratio was 11.12. A final difference Fourier was judged featureless; the largest peak (0.58 e/Å^3) was near a chlorine atom of the chloroform solvate. Final atomic coordinates are listed in Table I. Tables IS and IIS, tables of anisotropic temperature factors and fixed hydrogen atom coordinates, are available as supplementary material.

Results and Discussion

The crystal structure of $[Fe(TPP)(HIm)_2]Cl\cdot CHCl_3\cdot H_2O$ is comprised of two independent half ions of $[Fe(TPP)(HIm)_2]^+$ in the asymmetric unit of structure. The iron atom of each independent ion is located on an inversion center. Thus each ion has its two imidazole rings arranged in parallel orientations. Computer-drawn illustrations of each ion are shown in Figures 1 and 2. The most significant difference between the two ions is the orientation of the imidazole rings with respect to the porphinato core. The first ion has its imidazole ligands with ϕ angles of 5.7°; the second has ϕ angles of 41.4°. There is one other small, but significant, variation in the structures of the two ions that is related to the differing imidazole orientations (vide infra).

As noted in the introduction, crystalline $[Fe(TPP)(HIm)_2]Cl\cdot CHCl_3\cdot H_2O$ displays two overlapping normal low-spin EPR spectra. The two overlapping EPR spectra are thus seen to arise from two $[Fe(TPP)(HIm)_2]^+$ ions with slightly different geometries. The two ions effectively bracket the complete range of possible orientation angles for *parallel* imidazole planes. Importantly, neither extreme gives rise to an EPR signal that can be regarded as abnormal. Equally important is the demonstration that the changes in ligand orientation do give rise to experimentally distinguishable variations in "normal" EPR signals. The possibility that varying orientations of the axial imidazoles could be seen from EPR parameters has been previously discussed.[14] However, this

(13) $R_1 = \sum||F_o| - |F_c||/\sum|F_o|$ and $R_2 = [\sum w(|F_o| - |F_c|)^2/\sum w(F_o)^2]^{1/2}$.

Table I. Fractional Coordinates in the Unit Cell of $[Fe(TPP)(Im)_2]Cl\cdot H_2O\cdot CHCl_3$

atom	x	y	z
Fe(1)	0.0000	0.0000	0.0000
Fe(2)	0.5000	0.5000	0.5000
Cl(1)	0.49914 (18)	0.14346 (10)	0.07122 (22)
Cl(2)	0.16491 (22)	0.22280 (18)	0.00811 (22)
Cl(3)	0.22216 (26)	0.36701 (16)	0.0624 (3)
Cl(4)	0.1798 (4)	0.31495 (19)	0.25899 (24)
O(w)	0.4964 (3)	0.00083 (28)	0.1767 (4)
N(1)	0.00348 (23)	0.06980 (17)	−0.10735 (26)
N(2)	−0.10611 (23)	0.10101 (17)	0.11660 (26)
N(3)	0.11885 (26)	0.02983 (19)	0.09663 (28)
N(4)	0.2781 (3)	0.003202 (27)	0.1526 (4)
N(5)	0.63505 (22)	0.51962 (17)	0.47837 (27)
N(6)	0.41802 (22)	0.59975 (17)	0.44294 (27)
N(7)	0.48692 (23)	0.57296 (18)	0.67430 (28)
N(8)	0.48865 (29)	0.67965 (21)	0.8361 (3)
C(a1)	0.06558 (29)	0.04422 (23)	−0.2145 (3)
C(a2)	−0.0506 (3)	0.15510 (22)	−0.0869 (3)
C(a3)	−0.14651 (29)	0.18244 (22)	0.1079 (3)
C(a4)	−0.15386 (29)	0.10429 (22)	0.2234 (3)
C(a5)	0.73682 (28)	0.47423 (22)	0.5056 (3)
C(a6)	0.64752 (29)	0.58352 (22)	0.4409 (3)
C(a7)	0.45809 (29)	0.65390 (22)	0.4113 (3)
C(a8)	0.30920 (28)	0.62918 (21)	0.4277 (3)
C(b1)	0.0497 (3)	0.11472 (24)	−0.2603 (4)
C(b2)	−0.0210 (3)	0.18197 (24)	−0.1828 (4)
C(b3)	−0.2201 (3)	0.23581 (23)	0.2100 (4)
C(b4)	−0.2256 (3)	0.18793 (23)	0.2801 (4)
C(b5)	0.8125 (3)	0.50880 (26)	0.4805 (4)
C(b6)	0.7578 (3)	0.57520 (25)	0.4398 (4)
C(b7)	0.3707 (3)	0.71955 (24)	0.3805 (4)
C(b8)	0.2809 (3)	0.70410 (23)	0.3894 (4)
C(m1)	−0.1207 (3)	0.20811 (22)	0.0125 (4)
C(m2)	−0.13650 (29)	0.03717 (23)	0.2704 (3)
C(m3)	0.5637 (3)	0.64774 (22)	0.4102 (3)
C(m4)	0.23645 (29)	0.59481 (22)	0.4480 (3)
C(1)	−0.1718 (4)	0.29986 (25)	0.0183 (4)
C(2)	−0.2454 (4)	0.32275 (29)	−0.0696 (5)
C(3)	−0.2924 (5)	0.4063 (4)	−0.0670 (6)
C(4)	−0.2645 (8)	0.4661 (4)	0.0240 (8)
C(5)	−0.1942 (8)	0.4467 (4)	0.1123 (7)
C(6)	−0.1463 (5)	0.3613 (3)	0.1087 (5)
C(7)	−0.1974 (3)	0.05023 (23)	0.3854 (4)
C(8)	−0.2998 (4)	0.04761 (27)	0.3767 (4)
C(9)	−0.3552 (4)	0.0552 (3)	0.4810 (6)
C(10)	−0.3076 (5)	0.06420 (29)	0.5947 (6)
C(11)	−0.2067 (5)	0.0676 (3)	0.6060 (4)
C(12)	−0.1516 (3)	0.06173 (27)	0.5021 (4)
C(13)	0.2214 (4)	−0.00665 (29)	0.0690 (4)
C(14)	0.2104 (5)	0.0951 (4)	0.2388 (5)
C(15)	0.1123 (4)	0.0937 (3)	0.2053 (5)
C(16)	0.5906 (3)	0.71396 (24)	0.3756 (4)
C(17)	0.5838 (4)	0.7163 (3)	0.2532 (5)
C(18)	0.6036 (5)	0.7804 (4)	0.2225 (6)
C(19)	0.6301 (4)	0.8414 (3)	0.3139 (7)
C(20)	0.6381 (4)	0.83947 (29)	0.4338 (6)
C(21)	0.6178 (4)	0.77579 (26)	0.4666 (4)
C(22)	0.12290 (29)	0.63037 (24)	0.4121 (4)
C(23)	0.0928 (4)	0.5951 (3)	0.2935 (5)
C(24)	−0.0105 (5)	0.6269 (4)	0.2547 (6)
C(25)	−0.0834 (4)	0.6940 (4)	0.3343 (7)
C(26)	−0.0546 (4)	0.7303 (4)	0.4492 (7)
C(27)	0.0487 (4)	0.6978 (4)	0.4884 (5)
C(28)	0.4985 (3)	0.64808 (25)	0.7123 (4)
C(29)	0.4691 (4)	0.6234 (3)	0.8814 (4)
C(30)	0.4681 (4)	0.55760 (26)	0.7812 (4)
C(31)	0.2339 (6)	0.2785 (4)	0.1092 (7)

[a] The estimated standard deviations of the least significant digits are given in parentheses.

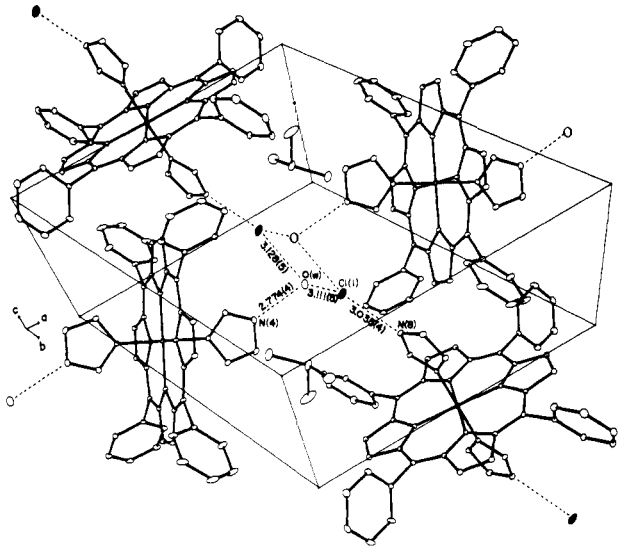

Figure 3. A diagram showing the hydrogen-bonding network found in the crystalline lattice of [Fe(TPP)(HIm)$_2$]Cl·CHCl$_3$·H$_2$O. The coordinates of the inversion center displayed in the center of the outline cell are $^1/_2$, 0, 0. All unique heavy-atom separations (with estimated standard deviations) in the hydrogen-bonding network are given.

is the first definitive proof of such orientation effects on the EPR spectra. Thus, in principle, the EPR spectra of bis(imidazole) hemes and hemoproteins (cytochromes *b*) can be interpreted in terms of varying geometries. The EPR parameters for three of the four limiting geometric cases are now available. The third case is that of a perpendicular alignment of the two ligand planes with a relatively large value for ϕ. The structure of an example of the third case is reported in the following paper.[10] The EPR spectrum of a complex having, unambiguously, an intermediate value of the interplanar dihedral angle remains wanting.

As noted in the introduction, the frozen solution EPR spectrum[11] of [Fe(TPP)(HIm)$_2$]Cl consists of a single normal signal almost identical with one of the two overlapping signals seen in the crystalline state. This suggests that one of the two rotational conformers in the crystal has a structure that is close to that found in solution. Our theoretical calculations[8] suggest that this will be the conformer with the small value of ϕ. Moreover, an examination of the crystal structure suggests a basis for the differing ϕ angles of the two ions in the solid state. Figure 3 illustrates the lattice arrangement and shows the two-dimensional hydrogen-bonding network that includes the imidazole N–H groups, the water molecule, and the chloride ion. The independent chloride ion and the water molecule are found close to the inversion center at $^1/_2$, 0, 0. Each water molecule is involved in forming two hydrogen bonds to the chloride ion, thus forming a central parallelogram around the inversion center.[15] As shown in the figure, the imidazole N–H (N(4)) forms a hydrogen bond to the water molecule with an N(4)···O(w) distance of 2.774 Å; the chain is continued by the inversion related N(4) hydrogen atoms.[16] The imidazoles of the second [Fe(TPP)(HIm)$_2$]$^+$ ion are involved in hydrogen bonds to the chloride ion with N(8)···Cl distances of 3.035 Å; this hydrogen bond system also continues in a quasilinear fashion. As shown in Figure 3, the two quasilinear hydrogen bond chains are approximately perpendicular to each other. Figure 3 also makes evident that, for the observed positions of the porphyrin macrocycles in the lattice, the 41° orientations of the imidazoles of the second ion are required for participation in the hydrogen bond network. Orientations of the ligands near 0° ϕ (with either Fe–N(5) or Fe–N(6)) would position the N(8) protons far away from the required hydrogen-bonding geometry.

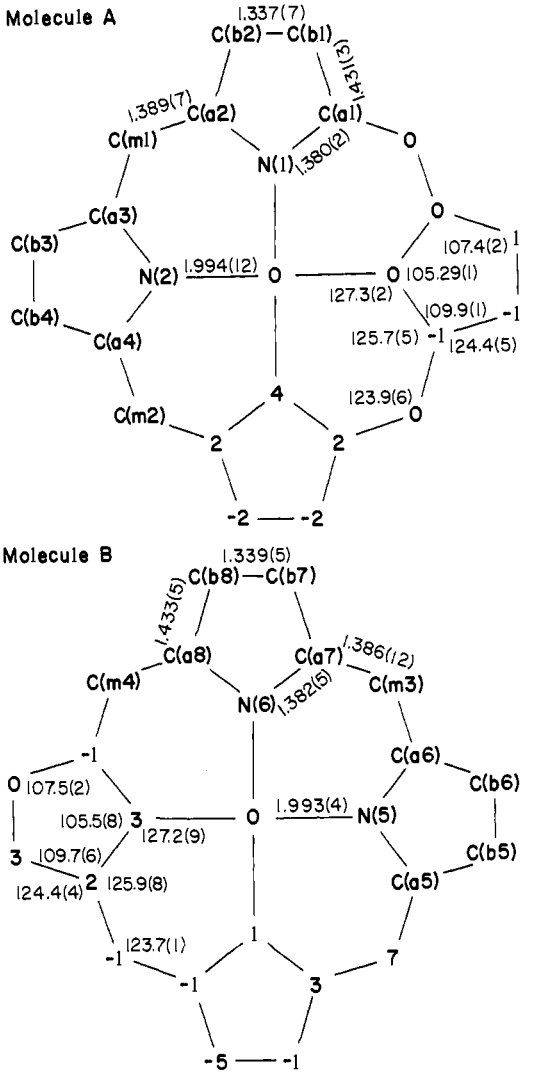

Figure 4. Formal diagrams of the porphinato cores in the two independent ions. (A) Values for the [Fe(TPP)(HIm)$_2$]$^+$ ion that has a ϕ angle of 6°; (B) values for the ion with ϕ = 41°. Each diagram gives averaged values for chemically distinct types within each respective ion. Both diagrams also display the perpendicular displacements (in units of 0.01 Å) of each crystallographically independent atom from the mean plane of the 24-atom core. The displacements of the centrosymmetrically related atoms are equal in magnitude and opposite in sign.

We have previously[9] tentatively concluded that the EPR signal with g_z = 2.84, g_y = 2.32, and g_x = 1.59 corresponds to the ion with ϕ = 5.7° and the signal with g_z = 3.00, $g_y \approx$ 2.2, and g_x = 1.47 to the ion with large ϕ. The calculated crystal field parameters have been given.[17] This assignment leads to the conclusion that the conformer with the small ϕ angle is thermodynamically favored.

Individual values of bond distances and angles are given in Tables II and III, respectively. Averaged values for each of the chemically unique types of bond distance and bond angle in the porphinato core are shown in parts A and B of Figure 4. The average values for each crystallographically independent ion are shown. Inspection of the diagrams shows that these averaged values are indistinguishable in the two half ions. Moreover, these averaged distances are the same as those reported[1] for the original crystalline phase of [Fe(TPP)(HIm)$_2$]Cl. Although the averaged

(14) Salerno, J. C.; Leigh, J. S. *J. Am. Chem. Soc.* **1984**, *106*, 2156–2159 and references cited therein.

(15) The Cl(1)–O(w)–Cl(1)′ angle is 101.1 (1)° and the O(w)–Cl(1)–O(w)′ angle is 78.9 (1)°. Note that the inversion center requires that the four internal angles of the parallelogram must sum to 360°.

(16) The unique hydrogen atom to heavy-atom separations in the network are the following: H(Ow1)–O(w) = 0.88 Å, H(Ow2)–O(w) = 0.91 Å, H(N4)···O(w) = 1.89 Å, H(N8)···Cl(1) = 2.19 Å, H(Ow1)···Cl(1) = 2.35 Å, H(Ow2)···Cl(1)′ = 2.23 Å.

(17) Crystal field parameters are Δ = 3.12 λ and V = 2.16 λ for the species with g_z = 2.84, g_y = 2.32, and g_x = 1.59 and Δ = 3.53 λ and V = 1.72 λ for the species with g_z = 3.00, $g_y \approx$ 2.2, and g_x = 1.47. See footnote 62 of ref 9.

Table II. Bond Distances in $[Fe(TPP)(Im)_2]Cl\cdot H_2O\cdot CHCl_3$

type	distances, Å	type	distances, Å
	Molecule A		
Fe(1)–N(1)	1.985 (3)	C(m1)–C(a3)	1.392 (5)
Fe(1)–N(2)	2.002 (3)	C(m1)–C(1)	1.509 (5)
Fe(1)–N(3)	1.977 (3)	C(m2)–C(a1)	1.398 (5)
N(1)–C(a1)	1.379 (5)	C(m2)–C(a4)	1.384 (5)
N(1)–C(a2)	1.381 (4)	C(m2)–C(7)	1.495 (5)
N(2)–C(a3)	1.383 (4)	C(1)–C(2)	1.382 (6)
N(2)–C(a4)	1.378 (4)	C(2)–C(3)	1.382 (7)
N(3)–C(13)	1.309 (5)	C(3)–C(4)	1.359 (11)
N(3)–C(15)	1.366 (5)	C(4)–C(5)	1.346 (11)
N(4)–C(13)	1.329 (5)	C(5)–C(6)	1.410 (8)
N(4)–C(14)	1.331 (6)	C(6)–C(1)	1.358 (7)
C(a1)–C(b1)	1.434 (5)	C(7)–C(8)	1.376 (5)
C(a2)–C(b2)	1.432 (5)	C(8)–C(9)	1.380 (7)
C(a3)–C(b3)	1.428 (5)	C(9)–C(10)	1.366 (8)
C(a4)–C(b4)	1.429 (5)	C(10)–C(11)	1.361 (7)
C(b1)–C(b2)	1.332 (5)	C(11)–C(12)	1.385 (6)
C(b3)–C(b4)	1.342 (5)	C(12)–C(7)	1.384 (5)
C(m1)–C(a2)	1.383 (5)	C(14)–C(15)	1.338 (7)
	Molecule B		
Fe(2)–N(5)	1.995 (3)	C(m4)–C(a5)	1.396 (5)
Fe(2)–N(6)	1.990 (3)	C(m4)–C(a8)	1.376 (5)
Fe(2)–N(7)	1.964 (3)	C(m4)–C(22)	1.498 (5)
N(5)–C(a5)	1.380 (4)	C(16)–C(17)	1.381 (6)
N(5)–C(a6)	1.385 (4)	C(17)–C(18)	1.392 (6)
N(6)–C(a7)	1.388 (4)	C(18)–C(19)	1.364 (8)
N(6)–C(a8)	1.376 (4)	C(19)–C(20)	1.349 (7)
N(7)–C(28)	1.324 (5)	C(20)–C(21)	1.401 (6)
N(7)–C(30)	1.368 (5)	C(21)–C(16)	1.376 (6)
N(8)–C(28)	1.325 (5)	C(22)–C(23)	1.376 (6)
N(8)–C(29)	1.353 (5)	C(23)–C(24)	1.384 (7)
C(a5)–C(b5)	1.432 (5)	C(24)–C(25)	1.355 (8)
C(a6)–C(b6)	1.426 (5)	C(25)–C(26)	1.342 (8)
C(a7)–C(b7)	1.437 (5)	C(26)–C(27)	1.388 (7)
C(a8)–C(b8)	1.436 (5)	C(27)–C(22)	1.350 (6)
C(b5)–C(b6)	1.342 (5)	C(29)–C(30)	1.348 (6)
C(b7)–C(b8)	1.335 (5)	C(31)–Cl(2)	1.694 (6)
C(m3)–C(a6)	1.397 (5)	C(31)–Cl(3)	1.753 (7)
C(m3)–C(a7)	1.375 (5)	C(31)–Cl(4)	1.721 (8)
C(m3)–C(16)	1.499 (5)		
	Hydrogen Bonding		
N(4)···O(ω)	2.774 (4)	O(ω)···Cl(1)	3.111 (5)
N(8)···Cl(1)′	3.035 (4)	O(ω)···Cl(1)″	3.128 (5)

[a] The numbers in parentheses are the estimated standard deviations. Primed and double primed atoms refer to the $1-x, 1-y, 1-z$ and $1-x, -y, -z$ transformations respectively.

Table III. Bond Angles in $[Fe(TPP)(Im)_2]Cl\cdot H_2O\cdot CHCl_3$

angles	degree	angles	degree
	Molecule A		
N(1)Fe(1)N(2)	89.85 (11)	N(2)C(a3)C(b3)	109.8 (3)
N(1)Fe(1)N(3)	89.36 (12)	N(2)C(a3)C(m1)	125.0 (3)
N(2)Fe(1)N(3)	90.19 (12)	C(b3)C(a3)C(m1)	125.1 (3)
Fe(1)N(1)C(a1)	127.06 (23)	N(2)C(a4)C(b4)	110.1 (3)
Fe(1)N(1)C(a2)	127.55 (24)	N(2)C(a4)C(m2)	125.8 (3)
C(a1)N(1)C(a2)	105.28 (28)	C(b4)C(a4)C(m2)	124.1 (3)
Fe(1)N(2)C(a3)	127.47 (24)	C(a1)C(b1)C(b2)	107.4 (3)
Fe(1)N(2)C(a4)	127.23 (22)	C(a2)C(b2)C(b1)	107.6 (3)
C(a3)N(2)C(a4)	105.30 (28)	C(a3)C(b3)C(b4)	107.5 (3)
Fe(1)N(3)C(13)	127.34 (29)	C(a4)C(b4)C(b3)	107.2 (3)
Fe(1)N(3)C(15)	127.8 (3)	C(a2)C(m1)C(a3)	124.3 (3)
C(13)N(3)C(15)	104.8 (4)	C(a2)C(m1)C(1)	117.8 (3)
C(13)N(4)C(14)	108.0 (4)	C(a3)C(m1)C(1)	118.0 (3)
N(1)C(a1)C(b1)	109.9 (3)	C(a1)′C(m2)C(a4)	123.5 (3)
N(1)C(a1)C(m2)′	126.2 (3)	C(a1)′C(m2)C(7)	117.0 (3)
C(b1)C(a1)C(m2)′	123.9 (3)	C(a4)C(m2)C(7)	119.4 (3)
N(1)C(a2)C(b2)	109.8 (3)	N(3)C(13)N(14)	111.0 (4)
N(1)C(a2)C(m1)	125.8 (3)	N(4)C(14)C(15)	106.4 (4)
C(b2)C(a2)C(m1)	124.4 (3)	N(3)C(15)C(14)	109.7 (5)
	Molecule B		
N(5)Fe(2)N(6)	89.36 (11)	C(b7)C(a7)C(m3)	124.5 (3)
N(5)Fe(2)N(7)	89.39 (12)	N(6)C(a8)C(b8)	109.4 (3)
N(6)Fe(2)N(7)	90.34 (12)	N(6)C(a8)C(m4)	126.5 (3)
Fe(2)N(5)C(a5)	126.58 (23)	C(b8)C(a8)C(m4)	124.0 (3)
Fe(2)N(5)C(a6)	128.39 (23)	C(a5)C(b5)C(b6)	107.4 (3)
C(a5)N(5)C(a6)	104.93 (28)	C(a6)C(b6)C(b5)	107.2 (3)
Fe(2)N(6)C(a7)	127.37 (23)	C(a7)C(b7)C(b8)	107.7 (3)
Fe(2)N(6)C(a8)	126.56 (233)	C(a8)C(b8)C(b7)	107.7 (3)
C(a7)N(6)C(a8)	106.07 (27)	C(a6)C(m3)C(a7)	123.6 (3)
Fe(2)N(7)C(28)	125.74 (26)	C(a6)C(m3)C(16)	118.1 (3)
Fe(2)N(7)C(30)	128.79 (25)	C(a7)C(m3)C(16)	118.3 (3)
C(28)N(7)C(30)	105.4 (3)	C(a5)″C(m4)C(a8)	123.8 (3)
C(28)N(8)C(29)	107.9 (3)	C(a5)″C(m4)C(22)	117.8 (3)
N(5)C(a5)C(b5)	110.0 (3)	C(a8)C(m4)C(22)	118.3 (3)
N(5)C(a5)C(m4)	125.7 (3)	N(7)C(28)N(8)	110.9 (4)
C(b5)C(a5)C(m4)	124.2 (3)	N(8)C(29)C(30)	106.4 (4)
N(5)C(a6)C(b6)	110.4 (3)	N(7)C(30)C(29)	109.3 (4)
N(5)C(a6)C(m3)	124.8 (3)	Cl(2)C(31)Cl(3)	108.0 (4)
C(b6)C(a6)C(m3)	124.9 (3)	Cl(2)C(31)Cl(4)	110.9 (4)
N(6)C(a7)C(b7)	109.0 (3)	Cl(3)C(31)Cl(4)	107.4 (4)
N(6)C(a7)C(m3)	126.4 (3)		

[a] The numbers in parentheses are the estimated standard deviations. Primed and double primed atoms refer to $-x, -y, -z$ and $1-x, 1-y, 1-z$ transformations, respectively.

values of Fe–N_p (1.993 (7) Å (this work) vs. the 1.989 (8) Å value previously reported) are experimentally indistinguishable and are in agreement with the average 1.990 Å value expected[18] for low-spin iron(III) complexes, there is an interesting pattern of Fe–N_p bond distances that correlates with axial ligand orientation. In the ion with the smaller value of ϕ, the two crystallographically unique Fe–N_p bond distances are 1.985 (3) and 2.002 (3) Å, a difference that appears to be experimentally significant. In the other ion, the two Fe–N_p bond distances are experimentally equivalent with individual values of 1.995 (3) and 1.990 (3) Å. The long bond distance in the first ion is the Fe–N_p bond that is eclipsed by the imidazole ligand; in the other ion with equivalent Fe–N_p bonds, neither bond is eclipsed. This rhombicity in the equatorial bond distances, as a function of axial ligand orientation, also appears to be present, but previously unrecognized, in other bis(imidazole) iron(III) derivatives. Thus in $[Fe(TPP)(HIm)_2]Cl\cdot CH_3OH$,[1] where the two ligands are 18 and 39° from the N1–N3 axis, these two bonds average to 1.993 (8) Å; the remaining two Fe–N_p bonds average to 1.985 (7) Å. In [Fe(Proto IX)(1-MeIm)$_2$]·$CH_3OH\cdot H_2O$,[3a] the pair of Fe–N_p bonds nearly eclipsed by the axial ligands (ϕ = 3 and 16°) average to 2.002 (14) Å; the other pair have an average value of 1.979 (9) Å. Although the statistical significance of these latter two examples is not absolute, given the current example the pattern is highly suggestive. If the effect is a consequence of axial ligand orientations, no effect is expected in $[Fe(TPP)(2\text{-MeHIm})_2]ClO_4$[10] where both sets of trans N–Fe–N bonds have identical environments. Indeed, both sets of Fe–N_p bonds are equivalent with averaged values of 1.972 (6) and 1.969 (4) Å. This static rhombicity in Fe–N_p bond parameters in one of the two crystallographically independent ions of $[Fe(TPP)(HIm)_2]Cl\cdot CHCl_3\cdot H_2O$ is also consistent with the two different EPR spectra.

We believe that this rhombicity results from π-bonding effects and competition between the porphyrin and axial ligands to π-donate to low-spin iron(III). As shown in our theoretical calculations,[8] the unpaired electron is expected to be in the d_π orbital perpendicular to the imidazole plane. Both the porphyrin and imidazole can π-donate electron density into this orbital but not to the other (filled) d_π orbital. The fact that the Fe–N_p bond parallel to this half-filled orbital is shorter implies that the porphyrin to Fe π bonding is significant. The other (filled) d_π orbital is of course relatively unaffected. Moreover, this same mechanism can explain the static distortion found in *high-spin* bis(imidazole) iron(III) complexes.

In $[Fe(OEP)(2\text{-MeHIm})_2]ClO_4$,[19] the two unique Fe–$N_p$ bond distances are 2.033 (1) and 2.049 (1) Å and in $[Fe(TPP)(BzHIm)_2]ClO_4$,[20] the two distances are 2.039 (4) and 2.059 (4)

(18) Scheidt, W. R.; Reed, C. A. *Chem. Rev.* **1981**, *81*, 543–555.

(19) Geiger, D. K.; Lee, Y. J.; Scheidt, W. R. *J. Am. Chem. Soc.* **1984**, *106*, 6339–6343.

Å. In both cases, the longer Fe–N_p bond is the one approximately perpendicular to the parallel imidazole planes. In high-spin iron(III) both of the relevant d_π orbitals are half filled. However, the porphyrin does not compete with imidazole for L to M π-donation with the orbital parallel to the imidazole planes. Hence, the porphyrin to Fe bonding is expected to be stronger in this direction and the Fe–N_p bond parallel to the imidazole planes is the shorter bond.[21,22]

The axial bond distances in the two independent ions of [Fe(TPP)(HIm)$_2$]Cl·CHCl$_3$·H$_2$O are also different. The length in ion A is 1.977 (3) Å, while the value in ion B is 1.964 (3) Å. The original report by Hoard et al.[1] provides the basis for expecting and understanding this effect. As pointed out by Hoard et al., the imidazole ligand with the smaller value of ϕ has more significant nonbonded interactions between axial ligand and the core and hence a longer axial bond distance is expected. These expectations are met in [Fe(TPP)(HIm)$_2$]Cl·CHCl$_3$·H$_2$O, and as noted, ion A has the smaller value of ϕ. The range of values for the axial bonds, previously observed, is from 1.957 to 1.991 Å.

Figure 4 also presents the displacements of the atoms from the mean plane of the respective 24-atom core. In neither ion are the deviations from planarity remarkable. The deviation from planarity of all units expected to be planar (imidazole rings, peripheral phenyls, and pyrrole rings) is less than 0.01 Å. The imidazole plane in ion A forms a dihedral angle of 86.4° with the porphyrin core; the corresponding value in ion B is 87.0°. The dihedral angles between the peripheral phenyl rings in ion A are 68.9 and 81.9°, and for ion B the values are 72.6 and 85.7°. There are no unusual intermolecular contacts.

Summary. The axial imidazole ligand orientation leads to effects in the lengths of the equatorial bonds in addition to the better-known correlation with the length of the axial bonds. This equatorial effect appears to result from competition between the porphyrin and imidazole to π-donate to the iron(III). The imidazole orientation effect also appears to lead to experimentally definable variations in the EPR spectrum and would allow, in principle, a definition of geometrical aspects of bis(imidazole) hemes and hemoproteins from the spectrum.

Note Added in Proof. Strouse et al.[23] have found that the low-spin complex bis(*cis*-methylurocanate)(*meso*-tetraphenylporphinato)iron(III) shows some similar effects. They find two different orientations of the parallel substituted imidazole ligands with ϕ = 16 and 29° and two overlapping "normal" EPR spectra. They have been able to fit the entire set of four observed ligand orientations and EPR spectra to a crystal field model. This study confirms our tentative assignments of EPR spectra with orientation angle. In addition, they observe a similar rhombicity of the equatorial Fe–N bond distances for the ϕ = 16° complex.

Acknowledgment. We thank the National Institutes of Health for support under Grant HL-15627 and Prof. F. A. Walker for useful discussions.

Registry No. [Fe(TPP)(HIm)$_2$]Cl, 25442-52-8.

Supplementary Material Available: Table IS, anisotropic temperature factors, and Table IIS, fixed hydrogen atom coordinates for [Fe(TPP)(HIm)$_2$]Cl·CHCl$_3$·H$_2$O (3 pages); listings of the observed and calculated structure amplitudes (×10) (19 pages). Ordering information is given on any current masthead page.

(20) Levan, K. R.; Strouse, C. E. *Abstract of Papers*: Americal Crystallolgraphic Association Summer Meeting, Snowmass, CO, Aug 1–5, 1983; Abstract H1. Levan, K. R. Ph.D. Thesis, UCLA, 1984.

(21) Note that the direction of the "back-bonding" mechanism in iron(III) porphyrinates is different for five- and six-coordinate high-spin iron(III) species. Six-coordinate derivatives have the same direction as low-spin iron(III) complexes.[22] Cf, Goff, H. M.; Shimomura, E. T.; Phillippi, M. A. *Inorg. Chem.* **1983**, *22*, 66–71.

(22) La Mar, G. N.; Walker, F. A. In *The Porphyrins*; Dolphin, D., Ed.; Academic Press: New York, 1979; Vol. IV, pp 61–157.

(23) Quinn, R.; Valentine, J. S.; Byrn, M. P.; Strouse, C. E. *J. Am. Chem. Soc.*, in press.

Unusual Orientation of Axial Ligands in Metalloporphyrins. Molecular Structure of Low-Spin Bis(2-methylimidazole)(*meso*-tetraphenylporphinato)iron(III) Perchlorate

W. Robert Scheidt,*[1] John F. Kirner, J. L. Hoard,*[2] and Christopher A. Reed*[3]

Contribution from the Departments of Chemistry, University of Notre Dame, Notre Dame, Indiana 46556, Cornell University, Ithaca, New York 14850, and the University of Southern California, Los Angeles, California 90089-1062. *Received October 15, 1986*

Abstract: The preparation and characterization of the low-spin complex [Fe(TPP)(2-MeHIm)$_2$]ClO$_4$ is described. The detailed temperature-dependent magnetic susceptibility of two different solvates and the crystal structure determination of the tetrahydrofuran solvate are reported. Solid samples of both solvates of [Fe(TPP)(2-MeHIm)$_2$]ClO$_4$ have an unusual low-spin EPR spectrum, the so-called "strong g_{max}" signal. This strong g_{max} signal is correlated with a mutually perpendicular alignment of the two axial 2-methylimidazole ligands. This arrangement solves certain stereochemical problems associated with the formation of the low-spin iron(III) complex with the sterically hindered axial ligands. In addition, the short axial bond required for the low-spin state is achieved by a tipping of the axial ligands and a substantial S_4 ruffling of the porphinato core. A detailed analysis and comparison of this structure and that of a related high-spin complex with the same axial ligands ([Fe(OEP)(2-MeHIm)$_2$]ClO$_4$) is given. This analysis shows the subtlety of the steric interactions of the methyl protons with porphinato core atoms. The axial Fe–N bond distance average is 2.012 Å, and the equatorial bond distance average is 1.970 Å. Crystal data for [Fe(TPP)(2-MeHIm)$_2$]ClO$_4$·THF·H$_2$O: monoclinic, a = 26.943 (3) Å, b = 16.927 (2) Å, c = 23.358 (3) Å, and β = 104.76 (1)°, Z = 8, space group $C2/c$, 6648 observed data.

The structural characterization of [Fe(TPP)(2-MeHIm)$_2$]ClO$_4$[4] was undertaken as part of our program to understand the control of structure, spin state, and other physical properties in (porphinato)iron species. As is well-known, (porphinato)iron(II) and

0002-7863/87/1509-1963$01.50/0